NJC

Dynamic Article Links

Cite this: DOI: 10.1039/c2nj40961e

www.rsc.org/njc

PAPER

Tuning conformations of calix[4]tubes by weak intramolecular interactions

Kirill Puchnin,[a] Dmitry Cheshkov,[ab] Pavel Zaikin,[a] Ivan Vatsouro*[a] and Vladimir Kovalev*[a]

Received (in Montpellier, France) 22nd October 2012, Accepted 27th October 2012
DOI: 10.1039/c2nj40961e

The conformational distribution in distally functionalized adamantylated calix[4]tubes was analyzed with NMR and quantum-chemical calculations. Without any intramolecular interactions, ester-, acid-, amino-, alcohol-, isocyanate-, phthalimide- and urea-substituted calixtubes preferred less sterically hindered *flattened cone* conformers in solution. In contrast, in a non-polar medium ($CDCl_3$) for calixtubes bearing two 3-carboxymethyl-1-adamantyl or 3-(2-ureidoethyl)-1-adamantyl units, the less sterically preferable *flattened cone* conformation with bulky substituents connected by intramolecular hydrogen bonds was found to be more favorable. On the other hand, for a calixtube with two positively charged units, only the conformer with distanced substituents was exclusively detected. Thus, the conformational equilibrium in functionalized calix[4]tubes can be controlled by intramolecular hydrogen bonding between appropriately arranged carboxylic groups or urea moieties, or by electrostatic repulsion of positively charged substituents.

Introduction

The control of macrocycle conformations is one of the most important parts in the design of calixarene-based receptors.[1] Despite the well-studied 'fixing' of a calix[4]arene core in one of four main conformations (*cone*, *partial cone*, 1,2-*alternate*, or 1,3-*alternate*) by simple introduction of bulky groups to the narrow rim, the internal conformational mobility of the macroring is not completely suppressed in most cases. When the *cone* conformation is mounted by four alkyl residues at the narrow rim, residual interconversion between two C_{2v}-symmetrical *flattened cone* conformers is fast on the NMR time scale and produces broadened spectra reflecting the time-averaged C_{4v} symmetry of the core.[2] The conformational motions can be more or less efficiently suppressed by intramolecular bridging,[3] guest (cation) complexation,[4] or by the grafting of several calixarene molecules into aggregates by covalent or weak intramolecular interactions.[5]

In calix[4]tubes (Fig. 1), which are unique quadruple-bridged bis-macrocycles first introduced by Beer and co-workers,[6] the calix[4]arene counterparts are greatly rigidified and possess C_{2v} symmetry not only in the solid state (that is common for most of *cone* calix[4]arene tetra-ethers) but also in solution as follows from characteristic signal doubling in ^1H and ^{13}C NMR spectra. Still, conformational interconversion is not blocked but is significantly decelerated in calixtubes, and exchange rates can be easily derived from EXSY experiments. For calixtubes **1–3**, representing different combinations of classical and thiacalixarenes, conformational exchange rate constants in $CDCl_3$ are 0.9 s^{-1} (328 K),[6b] 9.3 s^{-1} (273 K),[7] and 2.5 s^{-1} (328 K),[8] respectively. Removal or replacement of *tert*-butyl groups with different alkyl residues or halogens may alter the rate constants but keep

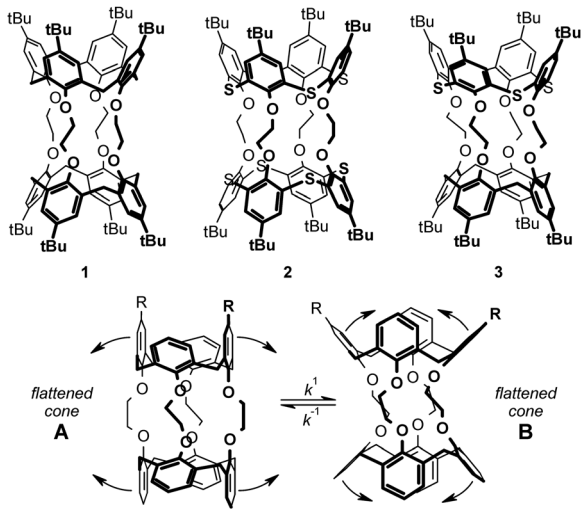

Fig. 1 Examples of classical (**1**), thia- (**2**), and hybrid (**3**) calix[4]tubes; conformational interconversions in calix[4]tubes.

[a] *Department of Chemistry, M.V. Lomonosov Moscow State University, Lenin's Hills, Moscow, 119991, Russia. E-mail: vatsouro@petrol.chem.msu.ru, kovalev@petrol.chem.msu.ru*
[b] *State Research Institute for Chemistry and Technology of Organoelement Compounds, 38, Sh. Entuziastov, Moscow, 105118, Russia*

them measurable by NMR at ambient or even elevated temperatures.[6b,c,7,8]

Recently we have prepared a series of calixtubes bearing substituted adamantanes at the wide rims, which have made available bis-macrocycles with different functional groups (esters, acids, amides, alcohols, amines and ureas).[9] Among them, a series of calixtubes with two distal functional units have been obtained. Due to, at least, different sterical crowding of the calixarene moieties, the disubstituted calixtubes have an unequal distribution of *flattened cone* conformers (**A** and **B**, Fig. 1), and for known selectively de-*tert*-butylated and halogenated calixtubes, less sterically hindered conformers **B** have been found dominant.[6b,c]

Herein we examined calixtubes **4–15** (Fig. 2) to assess the influence of functional groups on the conformational equilibrium, assuming that their possible interactions are competing forces to the steric hindrance of bulky units.

Results and discussion

Calixtubes **4**, **5**, **11–15** were obtained earlier,[9] and tubes **6–10** were prepared according to a scheme presented in Fig. 2, using approaches developed earlier for tetra-functionalized calixtubes.[9]

Despite the fact that for the previously known calixtubes with two bulky substituents the less sterically hindered conformer **B** was published to be the major one, the only conclusions made from NOESY were presented with no details of the structure analysis.[6b,c] To gain a tool for extracting conformer ratios of disubstituted calixtubes from ^{1}H NMR spectra, signals of the main conformer of diester **4**, as a representative example, in the spectra were completely assigned. After splitting the spectral pattern in the ^{1}H NMR spectrum of **4** into two sets by EXSY (Fig. 3a), the NOESY spectrum was collected at a lowered temperature (223 K) in $CDCl_3$ to suppress conformational motions and minimize contribution of the chemical exchange into the NOESY cross-peaks, and also to shift the equilibrium toward the more stable conformer (conformer ratio changed from 25/75 at 298 K to 10/90 at 223 K). The 2D NOESY spectrum was cut into slices through diagonal peaks and the NOE values were

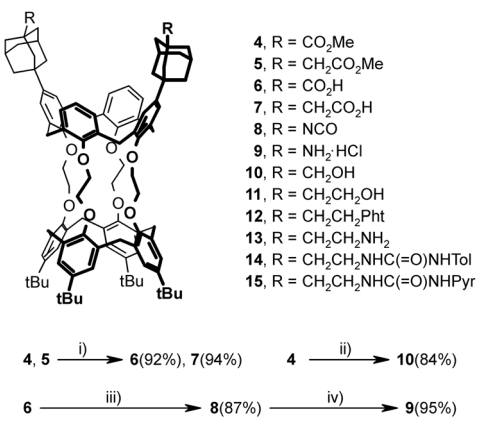

Fig. 2 Disubstituted calixtubes studied (Pht = *N*-phthalimide, Tol = 4-tolyl, Pyr = 1-pyrenyl). (i) nBu$_4$NOH/THF then HCl; (ii) $LiAlH_4$/THF; (iii) $SOCl_2$/benzene, then NaN_3/acetone/H_2O, then benzene/heating; (iv) HCl/dioxane.

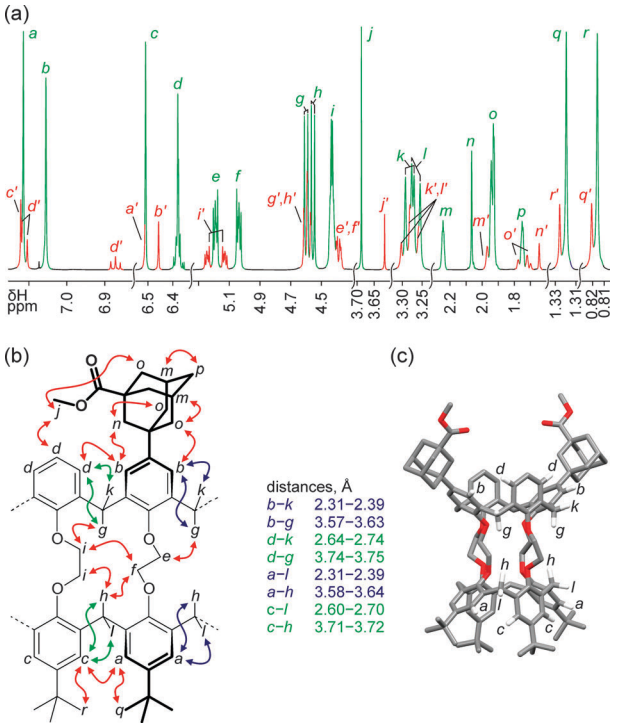

Fig. 3 (a) Parts of the 600 MHz ^{1}H NMR spectrum (scaled non-proportional) of diester **4** in $CDCl_3$ at 298 K: major conformer – *a–r*, green; minor conformer – *a′–r′*, red (from 2D EXSY); (b) NOEs in major conformer of **4** ($CDCl_3$, 223 K, t_{mix} 0.3 s); (c) energy-minimized structure of conformer **4B**.

derived by integration of the signals with the corresponding diagonal peak intensity set to 100% (Table 1, Fig. 3b). Measurement of the cross-peak volumes directly from the 2D spectrum gave the same numerical values of NOEs for well-resolved signals, but returned unreliable data for partly overlapped peaks.

Cross-peaks between *j*, *m*, *n*, *o*, *p* allowed assignment of the signals from the substituted adamantane units (confirmed by HSQC and ^{13}C NMR chemical shifts calculations by the additive scheme). Intensive NOEs *b–n* and *b–o* identified adamantylated aromatic units, and the far less intensive NOEs between *n*, *o*, *p* and *d* reflected the proximity of the adamantylated and unsubstituted calixarene aromatic moieties. From the NOEs *a–q* and *c–r*, the pairs of *tert*-butyl groups and calixarene aromatic rings were correlated. Intensive NOEs *a–l* and *c–l*, and the less intensive *a–h* and *c–h* showed *h* and *l* to be resonances from the axial and equatorial protons in the $ArCH_2Ar$ linkers in the *tert*-butylated calix[4]arene macrocycle, respectively. Analogously, methylene protons in the opposed calixarene macroring were identified from the NOEs *b–k*, *d–k*, *b–g*, and *d–g*.

Thus, nearly all signals in the ^{1}H NMR spectrum of the major conformer of diester **4** were assigned, except for those from the OCH_2CH_2O-linkers. As distances between the protons of the ethylene groups and the calixarene aromatics are too large, the assignments of *trans*- and *gauche*-OCH_2-CH_2O could not be done by NOESY. Next, the ^{13}C NMR spectrum of **4** was collected and resonances from the major conformer were fully assigned (see Experimental section) with HSQC and HMBC correlations. In particular, cross-peaks in

Table 1 Significant NOEs in diester **4**[a]

$H_{diagonal}$	H_{cross}	NOE	$H_{diagonal}$	H_{cross}	NOE
a	*c*	●●●●●	*i*	*e*	●●●
	h	●●●●		*f*	●●●
	l	●●●●●●		*g*	●●●●
	q	●●●●		*h*	●●●●
b	*d*	●●●●		*k* + *l*	●●●●
	g	●●●●	*j*	*d*	●
	k	●●●●●●		*o*	●
	n	●●●●	*k* + *l*	*a*	●●●●●
	o	●●●●●●		*b*	●●●●
	p	●		*c*	●●●
c	*a*	●●●●		*d*	●●●●
	h	●●●		*e*	●●●●
	l	●●●●		*f*	●●●●
	r	●●●●		*i*	●●●●●●
d	*b*	●●●	*m*	*o*	●●●●●●
	g	●●		*p*	●●●
	j	●	*n*	*b*	●●●
	k	●●●		*m*	●
e	*g*	●●●●●●		*o*	●●●●●
	h	●●●●●	*o*	*b*	●●
	i	●●●●●		*m*	●●●
	k + *l*	●●●●●●		*n*	●●
f	*g*	●●●●●		*p*	●●
	h	●●●●●	*p*	*m*	●●●
	i	●●●●●		*o*	●●●●●
	k + *l*	●●●●●●	*q*	*a*	●●
g + *h*	*a*	●●●●	*r*	*c*	●●
	b	●●●			
	c	●●●			
	d	●●●			
	e	●●●●●●			
	f	●●●●●●			
	i	●●●●●●			

[a] All NOEs are negative (have the same sign as diagonal peaks) and are shown as "●", "●●", "●●●", "●●●●", "●●●●●", "●●●●●●" for absolute values of <2, 2–5, 5–10, 10–15, 15–20, and >20%, respectively.

the HMBC spectrum allowed indirect correlation between pairs of aromatic and OCH_2CH_2O–protons (*a–f*, *b–e*, *c–i*, and *d–i*, Fig. 4) through the calixarene narrow rim aromatic quaternary carbons, thus completing the assignment of the ^{1}H NMR spectrum of **4**.

Molecular structures of **A** and **B** conformers of diester **4** were accessed by quantum-chemical calculations (DFT PBE/L1).[10] In both cases, distances between calixarene aromatic protons and protons of adjacent $ArCH_2Ar$-groups were clearly distinguishable for aromatic moieties of different inclination, and measured values of NOE *a–l*, *c–l*, *a–h*, *c–h*, *b–k*, *d–k*, *b–g*, and *d–g* were well-correlated with corresponding intramolecular distances only in conformer **4B** (Fig. 3c). So, the main conformer of diester **4** in $CDCl_3$ proved to be *flattened cone* **B** with ^{1}H NMR resonances *e* and *f* representing *trans*-OCH_2CH_2O-linkers, and resonance *i* – *gauche*-OCH_2CH_2O-linkers.

As follows from the data analysis, the **A**/**B** ratio in the disubstituted calixtubes can be easily derived from the relative intensities of the aromatic *d*/*d*′ (AB_2/AX_2 spin systems) or/and *b*/*b*′ (singlets) protons and verified, if resolved, from other signals in spectra (*e.g.*, from methoxy *j*/*j*′ and *tert*-butyl resonances *q*/*q*′, *r*/*r*′ in the case of **4**). Following this simple measurements, the conformer ratios for the calixtubes **4–15**

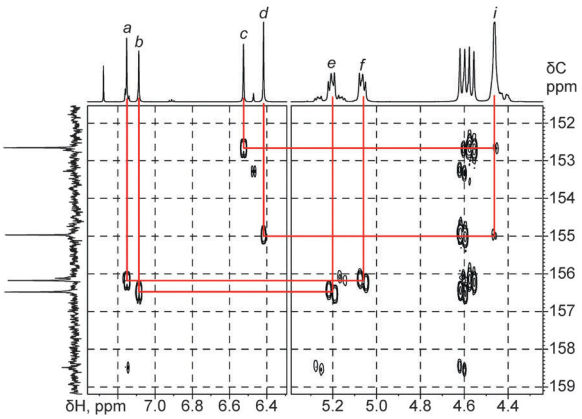

Fig. 4 Parts of HMBC spectrum of **4** ($CDCl_3$, 273 K) and ArH–OCH_2CH_2O-connections found (red lines).

were obtained (Table 2). As calixtubes **4**, **5**, **11–15** have been characterized only as potassium complexes,[9] the ^{1}H NMR spectra of their conformers **B** are also presented in the Experimental section.

In most cases, the less sterically hindered conformers **B** were found to be dominant. Also, adamantane units themselves seemed bulky enough to provide steric repulsions and stabilize conformer **B**, regardless of the size of the functional substituents: only small differences in the conformation distributions were observed for the calixtubes with ester, hydroxy, phthalimido and amino units.

This was not the case for diacid **7** and bis-ureas **14**, **15**. As follows from the ^{1}H NMR spectrum, in neat $CDCl_3$ (Fig. 5a) the major conformer of **7** was **A** with two bulky 3-carboxymethyl-1-adamantyl substituents located close to each other. This unexpected conformational distribution was maintained at different calixtube concentrations and was not drastically affected by the cooling or heating of the sample.

When several drops of CF_3CO_2D were added to the solution, the conformational distribution was reversed, and conformer **7B** became dominant (Fig. 5b, **7A**/**7B** = 25/75). The same effect was achieved by addition of DMSO-d_6 to a $CDCl_3$-solution of **7**. This behavior is consistent with the formation of internal hydrogen bonds, providing stabilization of the less sterically favorable conformer **7A** in non-polar medium.

The structures of the conformers of **7** were accessed by quantum-chemical calculations. First, the structure of conformer **7B** was optimized at the DFT PBE/L1 level,[10] then the structure of conformer **7A** was obtained from the calculated structure of conformer **7B** by a scanning procedure with gradual changing of the geometry of the calixtube core

Table 2 Conformers **A**/**B** ratios for **4–15** in $CDCl_3$ at 298 K[a]

Tube	**A**/**B** ratio	Tube	**A**/**B** ratio	Tube	**A**/**B** ratio
4	25/75	**8**	35/65	**12**	30/70
5	25/75	**9**	25/75[b]	**13**	35/65
6	35/65	**10**	25/75	**14**	50/50
7	75/25	**11**	35/65	**15**	50/50

[a] Accuracy ±5%. [b] Measured in CD_3OD due to insolubility of the salt in $CDCl_3$.

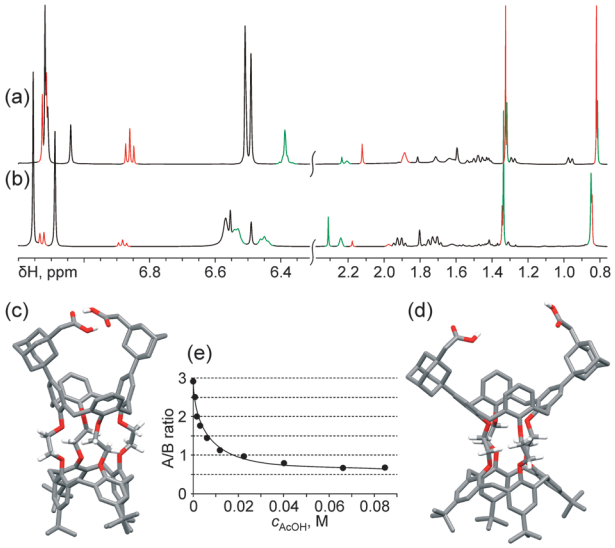

Fig. 5 Parts of the 600 MHz ^{1}H NMR spectra of **7** (scaled non-proportional) in neat $CDCl_3$ at 298 K (a) and after addition of CF_3CO_2D (b); signals used for **A**/**B** determination are colored red (**7A**) and green (**7B**); calculated structures of **7A** (c) and **7B** (d); **7A**/**7B** ratio at different concentrations of acetic acid in $CDCl_3$ (e).

from *flattened cone* **B** to *flattened cone* **A**, and finally the structures were optimized at the DFT B3LYP/6-31G level.[11] The results (Fig. 5c and d) showed that in conformer **7A** two co-facial carboxylic groups can form two hydrogen bonds, stabilizing the conformer and making it more favorable than conformer **7B**.[12] The same calculations were made for the homologous diacid **6** (Fig. 6), which showed that in conformer **6A** only one hydrogen bond can be formed between the non-coplanar carboxylic groups, thus allowing the steric repulsion to prevail over the bridging interactions. Still, the conformational equilibrium in **6**/$CDCl_3$ (as well as in cases of **8**, **11** and **13**) is a little bit shifted toward *flattened cone* **A**, if compared to the more sterically hindered calixtubes **4** and **5** having no interacting functional groups (see Table 2).

The stability of the hydrogen bonds in **7** was probed by NMR-titration with acetic acid, which was used instead of CF_3CO_2H as its concentration can be controlled more accurately and monitored by NMR. Upon increase of the solvent polarity, the **7A**/**7B** ratio dropped down smoothly with no intermittent changes, showing the gradual destabilization of conformer **7A** (Fig. 5e). The final **7A**/**7B** ratio reached in the $CDCl_3/CH_3CO_2H$ system was somewhat higher than that in $CDCl_3/CF_3CO_2D$ solution, which could be due to the uncomplete disruption of hydrogen bonds in the first case because of similar acidities of acetic acid and 1-adamantylacetic acid units in **7**.

In calixtubes **14** and **15**, with urea groups located in adamantane units, the **A**/**B** populations are nearly equal in $CDCl_3$ (Fig. 7a). Addition of CF_3CO_2D turned the conformational composition to **A**/**B** = 10/90 for both compounds (Fig. 7b), thus proving hydrogen bonding between the urea groups in non-competing medium; the titration experiment with acetic acid returned a plot similar to that presented in Fig. 5e for diacid **7**, with the final **14A**/**14B** value of 35/65. The 50/50 conformer ratio maintained at 273, 303 and 328 K (within the accuracy of measurements) in $CDCl_3$ resembled that of the tetra-substituted calixtubes, so it was supposed that in **14** and **15** the flexibly attached urea moieties may remain hydrogen bonded through all the conformational exchange processes between the energetically equal conformers.

As direct evidence of the hydrogen bonds maintenance was not available from the ^{1}H NMR spectra and NOESY correlations, quantum-chemical calculations were applied to judge if the mechanism of the conformational exchange includes hydrogen bonds breaking or not. Molecular structures of conformers **14A**, **14B**, and **14B′** sealed with hydrogen bonds (Fig. 7) were optimized first at the DFT PBE/L1 level,[10] and then by B3LYP/6-31G, and subjected to single point energy calculations at the B3LYP/Def2-TZVP level with the environment ($CHCl_3$) modelled by COSMO.[11] The results showed conformer **14A** to be more favorable than **14B** and **14B′**, and among the latter **14B** was more stable.

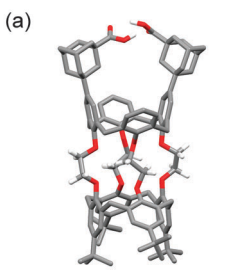

Fig. 6 Calculated structures of **6A** (a) and **6B** (b).

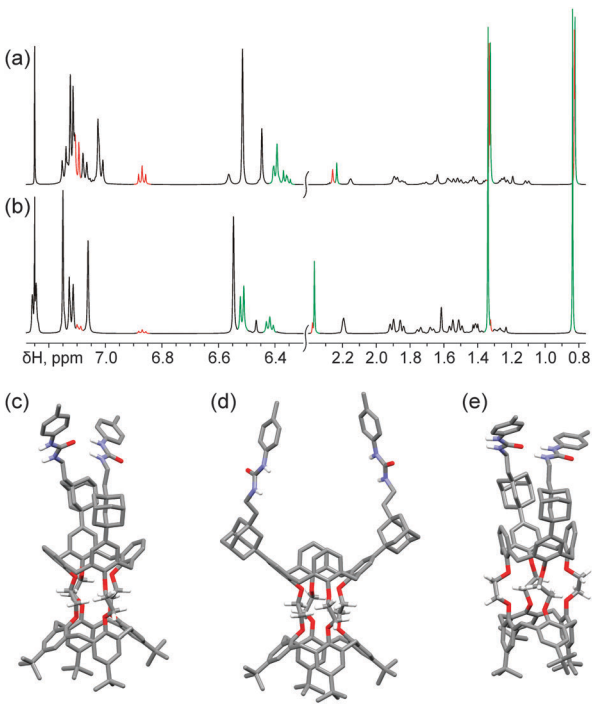

Fig. 7 Parts of the 600 MHz ^{1}H NMR spectra of **14** (scaled non-proportional) in neat $CDCl_3$ at 298 K (a) and after addition of CF_3CO_2D (b); signals used for **A**/**B** determination are colored red (**14A**) and green (**14B**). Calculated structures of conformers **14A** (c), **14B** (d), and **14B′** (e) with hydrogen bonds maintained.

Thus, the exchange **14A** ↔ **14B** seems to take place rather than **14A** ↔ **14B′**. Though all the integration approximations were switched off at the single point calculation step to minimize numerical errors, the energy differences between **14A** and **14B** (1.2 kcal mol^{-1}), and between **14A** and **14B′** (4.4 kcal mol^{-1}) are rather small, and one can say that they are below the trusted value for the method, so the presence of **14B′** in the mixture must not be completely excluded.

The outstandingly high (and equal) contents of conformers **14B** and **15B** (90%) in the $CDCl_3/CF_3CO_2D$ medium, and also the significant decrease of **14B** population when CF_3CO_2D was replaced with weaker acetic acid or DMSO, made it reasonable to suppose that the Coulomb repulsion of the protonated urea groups may contribute to the stability of conformers **14B** and **15B**. Such an effect was occasionally found in a pure form for calixtube **20** prepared from imidazophenanthrene-enriched calix[4]arene **18** and tetratosylate **19** (Scheme 1).

As pure **20** had an extremely broadened ^{1}H NMR spectrum in $CDCl_3$, it was converted into the protonated form by treatment with CF_3CO_2H. Surprisingly, the ^{1}H NMR spectrum of **20**·2H$^+$ was not only well-resolved, but it also contained signals from exclusively one conformer (Fig. 8). The conformer **B** structure of **20**·2H$^+$ was concluded from full assignment of the ^{1}H NMR spectrum with NOESY, which showed a *trans*-configuration of the OCH_2CH_2O units connected to imidazol-substituted calixarene moieties.

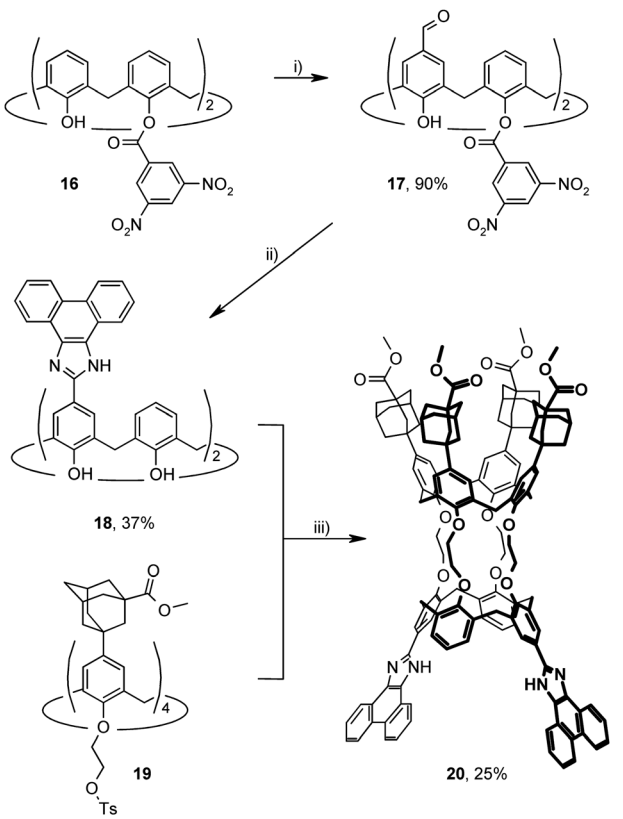

Scheme 1 Synthesis of imidazophenanthrene-containing calixtube **20**. (i) HMTA/TFA; (ii) 9,10-phenanthrenequinone/$CH_3CO_2NH_3$/CH_3CO_2H; (iii) K_2CO_3/*o*-xylene.

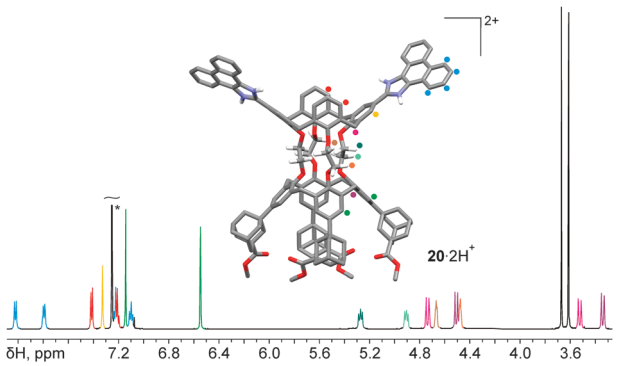

Fig. 8 Energy-minimized structure of protonated calixtube **20** (DFT PBE/L1) and a part of its 600 MHz ^{1}H NMR spectrum in $CDCl_3$ at 298 K with signal attribution.

Table 3 Exchange rate constants for calixtubes at 328 K[a]

Tube	Solvent	k^1, s^{-1} (**A** → **B**)	k^{-1}, s^{-1} (**B** → **A**)
4	$CDCl_3$	1.6	0.6
	$CDCl_3$ + CF_3CO_2D	1.4	0.4
7	$CDCl_3$	0.5	1.5
	$CDCl_3$ + CF_3CO_2D	1.7	0.8
14	$CDCl_3$	1.1	1.0
	$CDCl_3$ + CF_3CO_2D	1.0[b]	0.3[b]

[a] Measured from paired 2D EXSY correlations (t_{mix} 0 s, and t_{mix} 1 s). [b] Raw values due to significant cross-peaks overlap.

Thus, **20**·2H$^+$ represents the first calixtube system 'fixed' in a C_{2v}-symmetrical *flattened cone* conformation, and electrostatic repulsions were shown to be the force which, along with hydrogen bonding, can drastically affect the conformational equilibrium of the bis-macrocycles.

Finally, for calixtubes with functional groups capable of bonding interactions (**7**, **14**) and diester **4** (as a reference) the exchange rate constants were measured at 328 K (Table 3). As follows from the data, in neat $CDCl_3$ all the compounds possessed exchange rates that were quite similar to those known for classical calixtubes (at equal total concentrations of calixtubes), and neither bonding interactions nor addition of CF_3CO_2D altered the rates significantly.

Conclusions

A series of calixtubes with different functional groups located in distal positions of the upper rim was analyzed by NMR to assess the conformational behavior of the bis-macrocycles. It was found that the conformational distribution in calixtubes can be controlled or, at least, influenced by weak intramolecular interactions, such as hydrogen bonding or Coulomb repulsions, if appropriate substituents are introduced into the molecules. Still, these interactions did not alter the kinetics of the intramolecular exchange process. We hope, that these results will extend the applicability of calixtubes for the design of novel switchable supramolecular systems utilizing the unique ion-channel-like structure of the calixtube core.

Experimental

General methods and materials

NMR spectra were acquired on Bruker Avance 400 and Bruker Avance 600 instruments, and chemical shifts are reported as ppm referenced to solvent signals. In the ^{13}C NMR spectra, signal attribution was assisted with APT and DEPT135 experiments. MALDI-TOF mass spectra were run by using a Bruker AutoFlex II apparatus, and ESI mass spectra were obtained from an Agilent 1100 LC/MS system. Chemicals received from commercial sources were used without further purification. Solvents were purified and dried according to standard procedures. Calixtubes **4**, **5**, **11–15**, tetratosylate **19**[9] and calix[4]arene **16**[13] were synthesized according to published procedures. NMR spectra for the main conformers of known calixtubes are also presented, as they were characterized previously as potassium complexes only.

Synthesis and characterization

Diester 4. ^1H NMR [$CDCl_3$, 600 MHz, 303 K, main conformer (**B**)]: δ = 7.11 (s, 4H, ArH^{20}), 7.06 (s, 4H, ArH^{11}), 6.51 (s, 4H, ArH^{32}), 6.41–6.34 (m, 6H, $ArH^{24,25}$), 5.19 (m, 4H, $OCH_2{}^{15}$), 5.04 (m, 4H, $OCH_2{}^{16}$), 4.60 (d, 4H, J = 13.0 Hz, $ArCH_2Ar^{14,ax}$), 4.55 (d, 4H, J = 12.7 Hz, $ArCH_2Ar^{17,ax}$), 4.43 (m, 8H, $OCH_2{}^{28,29}$), 3.69 (s, 6H, $OCH_3{}^{1}$), 3.29 (d, 4H, J = 13.0 Hz, $ArCH_2Ar^{14,eq}$), 3.27 (d, 4H, J = 12.7 Hz, $ArCH_2Ar^{17,eq}$), 2.24 (m, 4H, $CH_{Ad}{}^{5}$), 2.07 (br s, 4H, $CH_{2\ Ad}{}^{8}$), 1.93 (m, 16H, $CH_{2\ Ad}{}^{4,7}$), 1.75 (m, 4H, $CH_{2\ Ad}{}^{6}$), 1.32 (s, 18H, $C(CH_3)_3{}^{23}$), 0.82 (s, 18H, $C(CH_3)_3{}^{35}$) ppm; ^{13}C NMR [$CDCl_3$, 151 MHz, 273 K, main conformer (**B**)]: δ = 178.25 (*2*), 156.35 (*13*), 156.04 (*18*), 154.83 (*27*), 152.52 (*30*), 144.58 (*21*), 144.18 (*33*), 143.39 (*10*), 135.12 (*12*), 135.03 (*19*), 133.15 (*26*), 131.73 (*31*), 127.93 (*25*), 125.40 (*20*), 125.09 (*11*), 124.73 (*32*), 122.37 (*24*), 72.91 (*15*), 72.78 (*16*), 72.18 (*28*,*29*), 51.80 (*1*), 44.37 (*8*), 42.25 (*7*), 41.81 (*3*), 38.04 (*4*), 35.79 (*9*), 35.55 (*6*), 34.05 (*22*), 33.47 (*34*), 32.41 (*14*), 32.06 (*17*), 31.66 (*23*), 30.92 (*35*), 28.62 (*5*) ppm.

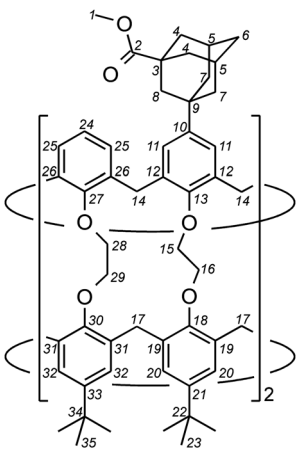

Diester 5. ^1H NMR [$CDCl_3$, 400 MHz, 303 K, main conformer (**B**)]: δ = 7.12 (s, 4H, ArH), 7.05 (s, 4H, ArH), 6.51 (s, 4H, ArH), 6.39 (br s, 6H, ArH), 5.19 (m, 4H, OCH_2), 5.05 (m, 4H, OCH_2), 4.60 (d, 4H, J = 13.1 Hz, $ArCH_2Ar$), 4.56 (d, 4H, J = 12.6 Hz, $ArCH_2Ar$), 4.44 (br s, 8H, OCH_2), 3.67 (s, 6H, OCH_3), 3.29 (d, 4H, J = 13.1 Hz, $ArCH_2Ar$), 3.27 (d, 4H, J = 12.6 Hz, $ArCH_2Ar$), 2.20 (br s, 8H, CH_2CO + CH_{Ad}), 1.94–1.46 (m, 24H, $CH_{2\ Ad}$), 1.33 (s, 18H, $C(CH_3)_3$), 0.82 (s, 18H, $C(CH_3)_3$) ppm.

Diacid 6. A mixture of diester **4** (0.65 g, 0.42 mmol), THF (45 mL) and aqueous nBu$_4$NOH (40%, 1 mL, 1.6 mmol) was stirred at reflux for 6 h. After cooling, the solvents were removed under reduced pressure, and the residue was treated with 5 M HCl. The solid formed was collected, washed repeatedly with water, and dried to afford pure **6** as a white solid (0.59 g, 92%). M.p. >300 °C; ^1H NMR [400 MHz, $CDCl_3$, 303 K, main conformer (**B**)]: δ = 7.11 (s, 4H, ArH), 7.04 (s, 4H, ArH), 6.50 (s, 4H, ArH), 6.36 (br s, 6H, ArH), 5.18 (m, 4H, OCH_2), 5.03 (m, 4H, OCH_2), 4.58 (d, 4H, J = 13.1 Hz, $ArCH_2Ar$), 4.55 (d, 4H, J = 12.6 Hz, $ArCH_2Ar$), 4.42 (br s, 8H, OCH_2), 3.26 (br d, 8H, J = 12.1 Hz, $ArCH_2Ar$), 2.26 (br s, 4H, CH_{Ad}), 2.17–1.65 (m, 24H, $CH_{2\ Ad}$), 1.31 (s, 18H, $C(CH_3)_3$), 0.81 (s, 18H, $C(CH_3)_3$) ppm; ESI-MS: m/z: 1572.4 $[M + K]^+$ for $C_{102}H_{116}KO_{12}$ (1572.8).

Diacid 7. A mixture of diester **5** (0.079 g, 0.05 mmol), THF (6 mL) and aqueous nBu$_4$NOH (20%, 0.26 mL, 0.20 mmol) was stirred at reflux for 6 h. After cooling, the solvents were removed under reduced pressure, and the residue was treated with 5 M HCl. The solid formed was collected, washed repeatedly with water, and dried to afford pure **7** as a white solid (0.073 g, 94%). M.p. > 300 °C; ^1H NMR [400 MHz, $CDCl_3$ + CF_3CO_2D, 298 K, main conformer (**B**)]: δ = 7.14 (s, 4H, ArH), 7.09 (s, 4H, ArH), 6.54 (s, 4H, ArH), 6.51 (br m, 6H, ArH), 5.31 (m, 4H, OCH_2), 5.06 (m, 4H, OCH_2), 4.67 (d, 4H, J = 13.0 Hz, $ArCH_2Ar$), 4.56 (d, 4H, J = 12.7 Hz, $ArCH_2Ar$), 4.43 (br s, 8H, OCH_2), 3.37 (d, 4H, J = 13.0 Hz, $ArCH_2Ar$), 3.29 (d, 4H, J = 12.7 Hz, $ArCH_2Ar$), 2.29 (s, 4H, CH_2CO), 2.22 (br s, 4H, CH_{Ad}), 1.89 (m, 8H, $CH_{2\ Ad}$), 1.78 (br s, 4H, $CH_{2\ Ad}$), 1.70 (m, 12H, $CH_{2\ Ad}$), 1.32 (s, 18H, $C(CH_3)_3$), 0.83 (s, 18H, $C(CH_3)_3$) ppm; ESI-MS: m/z: 1579.5 $[M + H_2O]^+$ for $C_{104}H_{120}O_{12}{\cdot}H_2O$ (1579.9).

Diisocyanate 8. A mixture of diacid **6** (0.31 g, 0.20 mmol), $SOCl_2$ (7.0 mL), dry benzene (7 mL) and pyridine (0.016 mL, 0.20 mmol) was carefully refluxed for 2 h. Excess $SOCl_2$ was removed by repeated re-evaporation with dry benzene under reduced pressure, and the residue was dissolved in dry acetone and cooled (ice). A solution of NaN_3 (0.26 g, 4.0 mmol) in water (1.0 mL) was added dropwise and the resultant mixture was stirred at cooling for 1 h and then kept in the fridge overnight. Water was added and the products were repeatedly extracted with CH_2Cl_2. Combined organic layers were washed with water, dried with $MgSO_4$, and evaporated under reduced pressure. The residue was dissolved in dry benzene (16 mL) and the solution was refluxed for 1.5 h. The solvent was removed to give pure **8** as a white solid (0.27 g, 87%). ^1H NMR [400 MHz, $CDCl_3$, 298 K, main conformer (**B**)]: δ = 7.11 (s, 4H, ArH), 7.02 (s, 4H, ArH), 6.51 (s, 4H, ArH), 6.38 (br s, 6H, ArH), 5.19 (m, 4H, OCH_2), 5.04 (m, 4H, OCH_2), 4.61 (d, 4H, J = 12.4 Hz, $ArCH_2Ar$), 4.55 (d, 4H, J = 12.7 Hz, $ArCH_2Ar$), 4.43 (br s, 8H, OCH_2), 3.28 (d, 4H, J = 12.7 Hz, $ArCH_2Ar$), 3.27 (d, 4H, J = 12.4 Hz, $ArCH_2Ar$), 2.30 (br s, 4H,

CH_{Ad}), 2.11–1.45 (m, 24H, $CH_{2\ Ad}$), 1.32 (s, 18H, $C(CH_3)_3$), 0.81 (s, 18H, $C(CH_3)_3$) ppm.

Diamine dihydrochloride 9. A mixture of diisocyanate **8** (0.27 g, 0.18 mmol), 1,4-dioxane (5 mL) and 2 M HCl (5 mL) was stirred at reflux for 8 h. After cooling the solid formed was collected, washed with dry ether and dried to give pure **9** as a white solid (0.26 g, 95%). M.p. >300 °C; ^{1}H NMR [400 MHz, CD_3OD, 298 K, main conformer (**B**)]: δ = 7.19 (s, 4H, ArH), 7.17 (s, 4H, ArH), 6.65–6.32 (m, 10H, ArH), 5.30 (m, 4H, OCH_2), 4.94 (m, 4H, OCH_2), 4.71 (d, 4H, J = 12.3 Hz, $ArCH_2Ar$), 4.59 (d, 4H, J = 12.5 Hz, $ArCH_2Ar$), 4.42 (br s, 8H, OCH_2), 3.37 (d, 4H, J = 12.5 Hz, $ArCH_2Ar$), 3.28 (d, 4H, J = 12.3 Hz, $ArCH_2Ar$), 2.40 (br s, 4H, CH_{Ad}), 2.10–1.64 (m, 24H, $CH_{2\ Ad}$), 1.34 (s, 18H, $C(CH_3)_3$), 0.85 (s, 18H, $C(CH_3)_3$) ppm; MALDI-MS: m/z: 1497.9 $[M + Na]^+$ for $C_{100}H_{118}NaN_2O_8$ (1497.9).

Diol 10. To the stirred suspension of $LiAlH_4$ (0.076 g, 2.0 mmol) in dry THF (10 mL) a solution of diester **4** (0.31 g, 0.20 mmol) in THF (10 mL) was added. The mixture was stirred at reflux for 3 h, cooled, and then water (0.08 mL), 3 M NaOH (0.08 mL) and water (0.24 mL) were added consecutively with stirring. The solid formed was filtered off, washed with THF, and the filtrate evaporated. The residue was washed with methanol to give pure **10** as a white solid (0.25 g, 84%). M.p. >300 °C; ^{1}H NMR [400 MHz, $CDCl_3$, 303 K, main conformer (**B**)]: δ = 7.12 (s, 4H, ArH), 7.07 (s, 4H, ArH), 6.51 (s, 4H, ArH), 6.39 (m, 6H, ArH), 5.18 (m, 4H, OCH_2), 5.04 (m, 4H, OCH_2), 4.60 (d, 4H, J = 12.9 Hz, $ArCH_2Ar$), 4.56 (d, 4H, J = 12.9 Hz, $ArCH_2Ar$), 4.44 (br s, 8H, OCH_2), 3.34 (s, 4H, $C\underline{H}_2OH$), 3.29 (d, 4H, J = 12.9 Hz, $ArCH_2Ar$), 3.27 (d, 4H, J = 12.9 Hz, $ArCH_2Ar$), 2.23 (br s, 4H, CH_{Ad}), 1.96–1.26 (m, 24H, $CH_{2\ Ad}$), 1.32 (s, 18H, $C(CH_3)_3$), 0.82 (s, 18H, $C(CH_3)_3$); ESI-MS: m/z: 1523.4 $[M + H_2O]^+$ for $C_{102}H_{120}O_{10}{\cdot}H_2O$ (1523.9) ppm.

Diol 11. ^{1}H NMR [400 MHz, $CDCl_3$, 303 K, main conformer (**B**)]: δ = 7.11 (s, 4H, ArH), 7.04 (s, 4H, ArH), 6.50 (s, 4H, ArH), 6.38 (m, 6H, ArH), 5.19 (m, 4H, OCH_2), 5.03 (m, 4H, OCH_2), 4.60 (d, 4H, J = 13.1 Hz, $ArCH_2Ar$), 4.55 (d, 4H, J = 12.6 Hz, $ArCH_2Ar$), 4.43 (br s, 8H, OCH_2), 3.78 (t, 4H, J = 7.5 Hz, $C\underline{H}_2OH$), 3.28 (d, 4H, J = 13.1 Hz, $ArCH_2Ar$), 3.26 (d, 4H, J = 12.6 Hz, $ArCH_2Ar$), 2.17 (br s, 4H, CH_{Ad}), 1.94–1.22 (m, 28H, $C\underline{H}_2CH_2OH + CH_{2\ Ad}$), 1.32 (s, 18H, $C(CH_3)_3$), 0.81 (s, 18H, $C(CH_3)_3$) ppm.

Diphthalimide 12. ^{1}H NMR [400 MHz, $CDCl_3$, 303 K, main conformer (**B**)]: δ = 7.82 (m, 4H, ArH_{Pht}), 7.68 (m, 4H, ArH_{Pht}), 7.10 (s, 4H, ArH), 7.04 (s, 4H, ArH), 6.50 (s, 4H, ArH), 6.39 (m, 6H, ArH), 5.19 (m, 4H, OCH_2), 5.04 (m, 4H, OCH_2), 4.60 (d, 4H, J = 13.1 Hz, $ArCH_2Ar$), 4.56 (d, 4H, J = 12.5 Hz, $ArCH_2Ar$), 4.43 (br s, 8H, OCH_2), 3.76 (m, 4H, NCH_2), 3.28 (d, 4H, J = 13.1 Hz, $ArCH_2Ar$), 3.26 (d, 4H, J = 12.5 Hz, $ArCH_2Ar$), 2.20 (br s, 4H, CH_{Ad}), 1.97–1.35 (m, 28H, $C\underline{H}_2CH_2N + CH_{2\ Ad}$), 1.31 (s, 18H, $C(CH_3)_3$), 0.81 (s, 18H, $C(CH_3)_3$) ppm.

Diamine 13. ^{1}H NMR [400 MHz, $CDCl_3$, 303 K, main conformer (**B**)]: δ = 7.11 (s, 4H, ArH), 7.04 (s, 4H, ArH), 6.50 (s, 4H, ArH), 6.39 (m, 6H, ArH), 5.18 (m, 4H, OCH_2), 5.03 (m, 4H, OCH_2), 4.59 (d, 4H, J = 13.1 Hz, $ArCH_2Ar$), 4.55 (d, 4H, J = 12.6 Hz, $ArCH_2Ar$), 4.43 (br s, 8H, OCH_2), 3.28 (d, 4H, J = 13.1 Hz, $ArCH_2Ar$), 3.26 (d, 4H, J = 12.6 Hz, $ArCH_2Ar$), 2.76 (m, 4H, NCH_2), 2.16 (br s, 4H, CH_{Ad}), 1.93–1.16 (m, 28H, $C\underline{H}_2CH_2N + CH_{2\ Ad}$), 1.31 (s, 18H, $C(CH_3)_3$), 0.81 (s, 18H, $C(CH_3)_3$) ppm.

Bisurea 14. ^{1}H NMR [600 MHz, $CDCl_3$ + CF_3CO_2D, 303 K, main conformer (**B**)]: δ = 7.25 (d, 4H, J = 8.3 Hz, ArH_{Tol}), 7.15 (s, 4H, ArH), 7.12 (d, 4H, J = 8.3 Hz, ArH_{Tol}), 7.06 (s, 4H, ArH), 6.55 (s, 4H, ArH), 6.52 (d, 4H, J = 7.5 Hz, ArH), 6.42 (t, 2H, J = 7.5 Hz, ArH), 5.23 (m, 4H, OCH_2), 5.06 (m, 4H, OCH_2), 4.66 (d, 4H, J = 13.1 Hz, $ArCH_2Ar$), 4.57 (d, 4H, J = 12.6 Hz, $ArCH_2Ar$), 4.43 (br s, 8H, OCH_2), 3.38 (m, 4H, NCH_2), 3.34 (d, 4H, J = 13.1 Hz, $ArCH_2Ar$), 3.29 (d, 4H, J = 12.6 Hz, $ArCH_2Ar$), 2.37 (s, 6H, CH_3), 2.19 (br s, 4H, CH_{Ad}), 1.88 (m, 8H, $CH_{2\ Ad}$), 1.71 (m, 4H, $CH_{2\ Ad}$), 1.61 (br s, 4H, $CH_{2\ Ad}$), 1.53 (m, 8H, $CH_{2\ Ad}$), 1.41 (m, 4H, $C\underline{H}_2CH_2N$), 1.34 (s, 18H, $C(CH_3)_3$), 0.84 (s, 18H, $C(CH_3)_3$) ppm.

Bisurea 15. ^{1}H NMR [600 MHz, $CDCl_3$ + CF_3CO_2D, 303 K, main conformer (**B**)]: δ = 8.35–7.90 (m, 18H, ArH_{Pyr}), 7.13 (s, 4H, ArH), 7.00 (s, 4H, ArH), 6.54 (s, 4H, ArH), 6.48 (d, 4H, J = 7.5 Hz, ArH), 6.37 (t, 2H, J = 7.5 Hz, ArH), 5.26 (m, 4H, OCH_2), 5.02 (m, 4H, OCH_2), 4.62 (d, 4H, J = 12.8 Hz, $ArCH_2Ar$), 4.54 (d, 4H, J = 12.5 Hz, $ArCH_2Ar$), 4.40 (br s, 8H, OCH_2), 3.37 (m, 4H, NCH_2), 3.30 (d, 4H, J = 12.8 Hz, $ArCH_2Ar$), 3.28 (d, 4H, J = 12.5 Hz, $ArCH_2Ar$), 2.09 (br s, 4H, CH_{Ad}), 1.79 (m, 8H, $CH_{2\ Ad}$), 1.62 (m, 4H, $CH_{2\ Ad}$), 1.52 (br s, 4H, $CH_{2\ Ad}$), 1.42 (m, 8H, $CH_{2\ Ad}$), 1.32 (s, 18H, $C(CH_3)_3$), 1.29 (m, 4H, $C\underline{H}_2CH_2N$), 0.83 (s, 18H, $C(CH_3)_3$) ppm.

Dialdehyde 17. A mixture of calixarene **16** (0.81 g, 1.0 mmol), HMTA (2.10 g, 15.0 mmol), and CF_3CO_2H (40 mL) was stirred at reflux (oil bath at 85 °C) for 24 h. After cooling, 2 M HCl (25 mL) was added and the products were extracted with CH_2Cl_2. Combined organic layers were washed with water, dried with $MgSO_4$ and evaporated to dryness. The residue was re-precipitated from CH_2Cl_2/hexane to give pure **17** as white solid (0.78 g, 90%). M.p. >200 °C (decomp); ^{1}H NMR (400 MHz, $CDCl_3$, 298 K): δ = 9.78 (s, 2H, CHO), 9.38 (d, 4H, J = 2.0 Hz, ArH_{Bzl}), 9.26 (t, 2H, J = 2.0 Hz, ArH_{Bzl}), 7.67 (s, 4H, ArH), 7.00 (br s, 6H, ArH), 5.86 (s, 2H, OH), 3.98 (d, 4H, J = 14.7 Hz, $ArCH_2Ar$), 3.74 (d, 4H, J = 14.7 Hz, $ArCH_2Ar$) ppm; MALDI-MS: m/z: 892.9 $[M + Na]^+$ for $C_{44}H_{28}NaN_4O_{16}$ (892.1).

Bis-imidazophenanthrene calix[4]arene 18. A mixture of calixarene **17** (0.87 g, 1.0 mmol), 9,10-phenanthrenequinone (0.50 g, 2.4 mmol), ammonium acetate (3.85 g, 50 mmol), and glacial acetic acid (50 mL) was heated with stirring at 120 °C for 6 h. After cooling, the solid formed was collected, washed with acetic acid, methanol, THF and dried to give pure **18** as a light purple solid (0.32 g, 37%). M.p. > 300 °C; ^{1}H NMR (400 MHz, DMSO[D_6], 298 K): δ = 8.91 (d, 4H, J = 8.8 Hz, ArH_{Phen}), 8.61 (d, 4H, J = 8.1 Hz, ArH_{Phen}), 8.00 (s, 4H, ArH), 7.81 (m, 4H, ArH_{Phen}), 7.72 (m, 4H, ArH_{Phen}), 7.17 (d, 4H, J = 7.6 Hz, ArH), 6.64 (t, 2H, J = 7.6 Hz, ArH), 4.17 (br s, 8H, $ArCH_2Ar$) ppm; ^{13}C NMR (100 MHz, DMSO[D_6], 298 K): δ = 159.67 br s, 153.12, 148.83, 131.23, 129.79 (C_{Ar}), 128.34 (CH_{Ar}), 127.87 (C_{Ar}), 127.48, 127.20, 126.34, 124.10,

122.12, 119.36 (CH_{Ar}), 114.51 (C_{Ar}), 32.31 ($ArCH_2Ar$) ppm; MALDI-MS: m/z: 856.9 $[M]^+$ for $C_{58}H_{40}N_4O_4$ (856.3).

Calixtube 20. A mixture of calixarene **18** (0.057 g, 0.066 mmol), calixarene **19** (0.138 g, 0.070 mmol), anhydrous K_2CO_3 (0.046 g, 0.333 mmol), and dry *o*-xylene (6.0 mL) was stirred at reflux for 60 h. After cooling, the reaction mixture was filtered, the solid was washed with CH_2Cl_2, and the combined organic solutions were evaporated to dryness. The residue was re-dissolved in CH_2Cl_2, washed with 10% aqueous acetic acid, water, brine, and then concentrated. Purification with column chromatography (SiO_2, gradient from CH_2Cl_2 to CH_2Cl_2/ethanol, 100 : 2) gave **20** as a gray solid (0.036 g, 25%). M.p. > 300 °C; ^{1}H NMR (600 MHz, $CDCl_3$ + CF_3CO_2D, 303 K): δ = 8.02 (d, 4H, J = 7.7 Hz, ArH_{Phen}), 7.79 (d, 4H, J = 7.7 Hz, ArH_{Phen}), 7.41 (d, 4H, J = 7.7 Hz, $ArH_{Calix\ H}$), 7.33 (s, 4H, $ArH_{Calix\ Phen}$), 7.22 (t, 4H, J = 7.7 Hz, ArH_{Phen}), 7.21 (t, 2H, J = 7.7 Hz, $ArH_{Calix\ H}$), 7.14 (s, 4H, $ArH_{Calix\ Ad}$), 7.10 (t, 4H, J = 7.7 Hz, ArH_{Phen}), 6.55 (s, 4H, $ArH_{Calix\ Ad}$), 5.27 (m, 4H, $ArOCH_{2\ Phen\ trans}$), 4.90 (m, 4H, $ArOCH_{2\ Ad\ trans}$), 4.74 (d, 4H, J = 14.0 Hz, $ArCH_2Ar_{Phen\ ax}$), 4.67 (m, 4H, $ArOCH_{2\ Phen\ gauche}$), 4.51 (d, 4H, J = 12.7 Hz, $ArCH_2Ar_{Ad\ ax}$), 4.47 (m, 4H, $ArOCH_{2\ Phen\ gauche}$), 3.67 (s, 6H, OCH_3), 3.61 (s, 6H, OCH_3), 3.52 (d, 4H, J = 14.0 Hz, $ArCH_2Ar_{Phen\ eq}$), 3.34 (d, 4H, J = 12.7 Hz, $ArCH_2Ar_{Ad\ eq}$), 2.24 (s, 4H, CH_{Ad}), 2.06 (s, 4H, CH_{Ad}), 2.00–1.22 (m, 48H, $CH_{2\ Ad}$) ppm; ^{13}C NMR (100 MHz, $CDCl_3$ + CF_3CO_2D, 298 K): δ = 181.49, 181.28 (C = O), 160.10, 158.33, 156.12, 152.72, 144.14, 143.13 (C_{Ar}), 136.99, 136.17 ($C_{Ar\ Phen}$), 135.43, 131.93 (C_{Ar}), 129.84 (CH_{Ar}), 128.29 ($C_{Ar\ Phen}$), 127.59 (CH_{Ar}), 127.35, 127.12 ($CH_{Ar\ Phen}$), 125.28 (CH_{Ar}), 125.10 ($C_{Ar\ Phen}$), 124.66 (CH_{Ar}), 123.52, 123.16 ($CH_{Ar\ Phen}$), 120.26 (CH_{Ar}), 73.24, 72.57, 72.18, 72.13 (OCH_2), 52.95, 52.85 (OCH_3), 41.26, 43.79, 42.80, 42.41, 42.13 ($CH_{2\ Ad}$), 41.73 (C_{Ad}), 37.91, 37.74, 36.04 ($CH_{2\ Ad}$), 35.50, 35.45, 35.34 (C_{Ad}), 32.19 ($ArCH_2Ar_{Phen}$), 31.91 ($ArCH_2Ar_{Ad}$), 28.72, 28.48 (CH_{Ad}) ppm; MALDI-MS: m/z: 2153.0 $[M]^+$ for $C_{142}H_{136}N_4O_{16}$ (2153.0).

Acknowledgements

This work was supported by Russian Foundation for Basic Research (projects 09-03-00971, 11-03-92006-HHC).

References

1 For comprehensive reviews on calixarene synthesis, properties and applications see: (*a*) V. Böhmer, Calixarenes, in *The Chemistry of Phenols*, ed. Z. Rappoport, John Wiley & Sons, Ltd, Chichester, 2003, pp. 1369–1454; (*b*) C. D. Gutsche, *Calixarenes, An Introduction*, Royal Society of Chemistry, Cambridge, UK, 2008; (*c*) *Calixarenes 2001*, ed. Z. Asfari, V. Böhmer, J. M. Harrowfield and J. Vicens, Kluwer Academic Publishers, Dordrecht, 2001; (*d*) *Calixarenes in the Nanoworld*, ed. J. Vicens, J. Harrowfield and L. Backlouti, Springer, Dordrecht, 2007.

2 In the case of calix[4]arenes 'flattened cone' is equal to 'pinched cone'. For experimental evidences and the interconversion barrier for the simplest case see: (*a*) A. Soi, W. Bauer, H. Mauser, C. Moll, F. Hampel and A. Hirsch, *J. Chem. Soc., Perkin Trans. 2*, 1998, 1471–1478; (*b*) A. Ikeda and S. Shinkai, *Chem. Rev.*, 1997, **97**, 1713–1734, and references therein.

3 Probably, the most efficient rigidification of the calix[4]arene core was achieved by the introduction of two short diethylene glycol bridges onto a narrow rim, that affected drastically the binding and aggregation abilities of the calixarene derivatives by bringing the core to nearly perfect C_{4v} symmetry: (*a*) A. Arduini, A. Casnati, L. Dodi, A. Pochini and R. Ungaro, *Chem. Commun.*, 1990, 1597–1598; (*b*) A. Arduini, M. Fabbi, M. Mantovani, L. Mirone, A. Pochini, A. Secchi and R. Ungaro, *J. Org. Chem.*, 1995, **60**, 1454–1457; (*c*) A. Arduini, V. Böhmer, L. Delmau, J.-F. Desreux, J.-F. Dozol, M. A. G. Carrera, B. Lambert, C. Musigmann, A. Pochini, A. Shivanyuk and F. Ugozzoli, *Chem.–Eur. J.*, 2000, **6**, 2135–2144; (*d*) A. Arduini, E. Brindani, G. Giorgi, A. Pochini and A. Secchi, *J. Org. Chem.*, 2002, **67**, 6188–6194; (*e*) G. Arena, A. Contino, E. Longo, G. Spoto, A. Arduini, A. Pochini, A. Secchi, C. Massera and F. Ugozzoli, *New J. Chem.*, 2004, **28**, 56–61; (*f*) M. O. Vysotsky, O. Mogck, Y. Rudzevich, A. Shivanyuk, V. Böhmer, M. S. Brody, Y. L. Cho, D. M. Rudkevich and J. Rebek Jr., *J. Org. Chem.*, 2004, **69**, 6115–6120; (*g*) I. Vatsouro, V. Rudzevich and V. Böhmer, *Org. Lett.*, 2007, **9**, 1375–1377.

4 Calix[4]arene rigidification at cation complexation was first established for calixarene tetraamides and tetraesters: (*a*) A. Arduini, E. Ghidini, A. Pochini, R. Ungaro, G. Andreetti, G. Calestani and F. Ugozzoli, *J. Inclusion Phenom.*, 1988, **6**, 119–134; (*b*) P. Guilbaud, A. Varnek and G. Wipff, *J. Am. Chem. Soc.*, 1993, **115**, 8298–8312; (*c*) A. Yamada, T. Murase, K. Kikukawa, T. Arimura and S. Shinkai, *J. Chem. Soc., Perkin Trans. 2*, 1991, 793–797; (*d*) G. Horvat, V. Stilinović, T. Hrenar, B. Kaitner, L. Frkanec and V. Tomišić, *Inorg. Chem.*, 2012, **51**, 6264–6278. See also ref. 6–9.

5 For selected recent data on bis-calixarenes (except for calixtubes) and calix(resorcin)arene dimers/oligomers see: (*a*) H. Dube and J. Rebek Jr., *Angew. Chem., Int. Ed.*, 2012, **51**, 3207–3210; (*b*) W. Hu, C. Blecking, M. Kralj, L. Šuman, I. Piantanida and T. Schrader, *Chem.–Eur. J.*, 2012, **18**, 3589–3597; (*c*) S. Slovak and Y. Cohen, *Chem.–Eur. J.*, 2012, **18**, 8515–8520; (*d*) H. Gan and B. C. Gibb, *Chem. Commun.*, 2012, **48**, 1656–1658; (*e*) H. Tang, C. Santos de Oliveira, G. Sonntag, C. L. D. Gibb, B. C. Gibb and C. Bohne, *J. Am. Chem. Soc.*, 2012, **134**, 5544–5547; (*f*) S. Pasquale, S. Sattin, E. Escudero-Adán, M. Martínez-Belmonte and J. de Mendoza, *Nat. Commun.*, 2012, **3**, 785; (*g*) A. Lledó, S. Kamioka, A. C. Sather and J. Rebek Jr., *Angew. Chem., Int. Ed.*, 2011, **50**, 1299–1301; (*h*) Z. Lin, T. J. Emge and R. Warmuth, *Chem.–Eur. J.*, 2011, **17**, 9395–9405; (*i*) L. Avram, Y. Cohen and J. Rebek Jr., *Chem. Commun.*, 2011, **47**, 5368–5375; (*j*) V. Rudzevich, O. Kasyan, A. Drapailo, M. Bolte, D. Schollmeyer and V. Böhmer, *Chem.–Asian J.*, 2010, **5**, 1347–1355; (*k*) Y. Rudzevich, V. Rudzevich and V. Böhmer, *Chem.–Eur. J.*, 2010, **16**, 4541–4549.

6 (*a*) P. Schmitt, P. D. Beer, M. G. B. Drew and P. D. Sheen, *Angew. Chem., Int. Ed. Engl.*, 1997, **36**, 1840–1842; (*b*) S. E. Matthews, P. Schmitt, V. Felix, M. G. B. Drew and P. D. Beer, *J. Am. Chem. Soc.*, 2002, **124**, 1341–1353; (*c*) S. E. Matthews, V. Felix, M. G. B. Drew and P. D. Beer, *Org. Biomol. Chem.*, 2003, **1**, 1232–1239.

7 S. E. Matthews, V. Felix, M. G. B. Drew and P. D. Beer, *New J. Chem.*, 2001, **25**, 1355–1358.

8 E. Khomich, M. Kashapov, I. Vatsouro, E. Shokova and V. Kovalev, *Org. Biomol. Chem.*, 2006, **4**, 1555–1560.

9 K. Puchnin, P. Zaikin, D. Cheshkov, I. Vatsouro and V. Kovalev, *Chem.–Eur. J.*, 2012, **18**, 10954–10968.

10 (*a*) D. N. Laikov, *Chem. Phys. Lett.*, 1997, **281**, 151–156; (*b*) D. N. Laikov and Y. A. Ustynyuk, *Russ. Chem. Bull.*, 2005, **54**, 820–826 (Quantum-chemical program PRIRODA); (*c*) J. P. Perdew, K. Burke and M. Ernzerhof, *Phys. Rev. Lett.*, 1996, **77**, 3865–3868 (PBE functional); (*d*) D. N. Laikov, *Chem. Phys. Lett.*, 2005, **416**, 116–120 (L1 basis set).

11 (*a*) ORCA program package, release 2.9.0; (*b*) W. J. Hehre, R. Ditchfield and J. A. Pople, *J. Chem. Phys.*, 1972, **56**, 2257–2261 (6-31G basis set); (*c*) A. Schaefer, H. Horn and R. Ahlrichs, *J. Chem. Phys.*, 1992, **97**, 2571–2577; (*d*) F. Weigend and R. Ahlrichs, *Phys. Chem. Chem. Phys.*, 2005, **7**, 3297–3305 (TZV basis sets); (*e*) S. Sinnecker, A. Rajendran, A. Klamt, M. Diedenhofen and F. Neese, *J. Phys. Chem. A*, 2006, **110**, 2235–2245 (COSMO implementation).

12 The calculated energy difference of 6 kcal mol^{-1} was at the level of the accuracy of the method, and more precise calculations may be performed, if needed, to ascribe the equilibrium quantitatively and get the energy barrier of **7A** ↔ **7B** exchange.

13 K. A. See, F. R. Fronczek, W. H. Watson, R. P. Kashyap and C. D. Gutsche, *J. Org. Chem.*, 1991, **56**, 7256–7268.

